PAPER • OPEN ACCESS

Medium-range percolation in two dimensions

View the article online for updates and enhancements.

IOP **ebooks**™

Bringing you innovative digital publishing with leading voices to create your essential collection of books in STEM research.

Start exploring the collection - download the first chapter of every title for free.

Medium-range percolation in two dimensions

Youjin Deng [1], Yunqing Ouyang [1] and Henk W J Blöte [2]

[1] Hefei National Laboratory for Physical Sciences at Microscale, Department of Modern Physics, University of Science and Technology of China, Hefei 230027, China
[2] Lorentz Institute, Leiden University, P.O. Box 9506, 2300 RA Leiden, The Netherlands

E-mail: `yjdeng@ustc.edu.cn`

Abstract. We investigate equivalent-neighbor percolation models in two dimensions with a variable interaction range, and include the mean-field limit. We employ a Monte Carlo algorithm whose efficiency depends only weakly on the number of equivalent neighbors within the range of the interactions. We consider 2 classes of models, one in which the interacting neighbors fill a circle, and one in which they fill a square. We first determine the critical points, and then determine the critical exponents. These are, for all finite ranges investigated, in agreement with the exactly known exponents of the nearest-neighbor model.

1. Introduction

It is well known that the scaling properties of models with long-range interactions reveal some aspects that are absent in short-range models, in particular the violation of hyperscaling. These aspects were analyzed in detail by Knops et al. [1] for the Ising model, using position-space renormalization. They found that these models can still be described by the renormalization theory, by use of the mechanism of dangerous irrelevant variables, i.e., singular dependence of the scaling function on these irrelevant fields.

In this work we place the percolation model in the wider context of the q-state Potts [2] model, for which a general theoretical context is available, as well as numerical results for $q = 2$, 3 and 4. The crossover between the mean-field (MF) Ising model ($q = 2$) and the short-range Ising model was numerically investigated by Luijten et al. [3]. It was found that, in two dimensions, all equivalent-neighbor Ising models with a finite range belong to the short-range universality class. Only the limit of infinitely many neighbors is mean-field-like. This result fits well with the principle that the universal properties of a phase transition are typically independent on the microscopic details of the Hamiltonian. Nevertheless, there are instances of models disobeying this principle. For instance, a seemingly innocent increase of the range of interactions to $\sqrt{5}$ times the nearest-neighbor distance turns the critical transition of the two-dimensional, 4-state Potts model into a discontinuous one [4]. Also the phase transition of the three-state Potts model becomes discontinuous for a sufficiently long range. The critical and first-order ranges are separated by a tricritical point located near the model with 80 equivalent neighbors [4].

These existing results for the $q = 2$ (Ising), and the $q = 3$ and 4 Potts models still have to be supplemented with a numerical analysis for the $q \to 1$ limit of the random-cluster model, i.e., the percolation model. In the present work, we investigate the role of the range of interactions in the two-dimensional percolation model. More specifically we consider equivalent-neighbor models, in which each site equally interacts with a local environment, i.e., a set of neighbors

filling a region around that site. We distinguish two cases of such local environments: first, we define the type-1 models, with local interactions between a site and all neighboring sites within a circle of radius r; and second, we define type-2 models with interactions including all neighboring sites within a $2r \times 2r$ square. More precisely, in type-1 models a site i with coordinates x_i, y_i couples to all sites j satisfying $\sqrt{(x_i - x_j)^2 + (y_i - y_j)^2} \leq r$, and in type-2 models to all sites j simultaneously satisfying $|x_i - x_j| \leq r$ and $|y_i - y_j| \leq r$.

We formulate this percolation problem using the language of the q-state Potts model and the equivalent random-cluster model [5]. The Potts variables s_k can, for all sites k assume the values $1, 2, \ldots, q$. The Potts Hamiltonian is

$$\mathcal{H} = -K \sum_{<i,j>} \delta(s_i, s_j) - H \sum_{k=1}^{N} \delta(s_k, 1) , \tag{1}$$

where the sum on $< i, j >$ is as defined above for cases 1 or 2. We restrict ourselves to the ferromagnetic case $K > 0$. The Kasteleyn-Fortuin mapping [5] involves the definition of bond variables with values $b_{ij} = 0$ or 1 between all site pairs i, j fitting within the interaction range r. In the absence of the external field H, summation of the Potts partition sum on the Potts variables then leads to the random-cluster partition sum

$$Z_{\mathrm{RC}} = \sum_{\mathcal{G}} (e^K - 1)^{N_{\mathrm{b}}} q^{N_{\mathrm{c}}} , \tag{2}$$

where the graph $\mathcal{G}$ is the set of bond variables with $b_{ij} = 1$, N_{b} is the sum over all b_{ij}, and N_{c} the number of percolating clusters formed by the graph $\mathcal{G}$. The connection with the percolation problem is obtained by setting $q = 1$ and dividing out a factor $e^{-KN_{\mathrm{e}}}$ where N_{e} is the total number of bond variables:

$$Z_{\mathrm{perc}} = e^{-KN_{\mathrm{e}}} Z_{\mathrm{RC}} \sum_{\mathcal{G}} p^{N_{\mathrm{b}}} (1-p)^{N_{\mathrm{e}} - N_{\mathrm{b}}} q^{N_{\mathrm{c}}} , \tag{3}$$

with $p = 1 - e^{-K}$. This sum is trivial for $q = 1$, but it may serve as the generating function of percolation configurations. Differentiation to q at $q = 1$ leads to the expectation value of the number of clusters N_{c}. The relation between the Potts magnetic properties and the cluster-size distribution of the percolation model also requires the $q \to 1$ limit [6] of the random-cluster model.

The physics of the medium-range percolation model was recently investigated by Ouyang et al. [7], using a Monte Carlo method, and subsequent analysis of the Binder [8] ratio and the wrapping probabilities. The present work includes several new models, and, in addition explores the scaling behavior of the wrapping probabilities as defined by Scullard and Jacobsen [9]. These wrapping probabilities display very favorable scaling properties for planar lattices. Furthermore, it has been shown [10] that non-planar bonds introduce only rather weak corrections to scaling. Therefore, it seems worthwhile to analyze the Scullard-Jacobsen wrapping probabilities in the present non-planar medium-range models.

2. Computational aspects
2.1. Simulation method
All simulations were performed on square lattices with periodic boundary conditions. The Monte Carlo generation of bond percolation configurations involves the placing of bond variables with probability p. This can be done by computing a uniformly distributed random number X, for

instance in the range $0 < X \leq 1$, and placing a bond if $X < p$. Typical values of p are $p \approx 1/z$. For models with a large number z of interacting neighbors, for instance $z = 4016$, one thus would typically have to compute thousands of random numbers before a bond can be placed. A more efficient approach is to analytically compute the probability $P(j) = (1 - p)^{j-1} p$ that the jth interacting neighbor is the first one to be connected by the bond selection process [11]. The cumulative distribution of the first selected neighbor is then

$$C(k) = \sum_{j=1}^{k} P(k) = 1 - (1 - p)^k \qquad (4)$$

The number k can thus be obtained from X by the condition

$$C(k-1) \leq X \leq C(k), \qquad (5)$$

which requires a number of operations of order 1 instead of z.

2.2. Sampled quantities

After completion of the random process of defining the bond variables b_{ij}, the graph $\mathcal{G}$ is decomposed in disconnected clusters. For each graph $\mathcal{G}$ thus generated, we sampled the density c_l of the largest cluster, the sum $\sum_i c_i^2$ of the squared cluster densities, and $\sum_i c_i^4$ of the fourth powers. The cluster decomposition allows the sampling of magnetic quantities in the random-cluster model. In the Ising case $q = 2$, the expectation values of the second and fourth moments of the magnetization density satisfies

$$\langle m^2 \rangle = \left\langle \sum_i c_i^2 \right\rangle, \quad \langle m^4 \rangle = \left\langle 3 \left(\sum_i c_i^2 \right)^2 - 2 \sum_i c_i^4 \right\rangle, \qquad (6)$$

and thus the Binder ratio of an $L \times L$ system, at a distance t to the critical point, can be expressed as

$$Q(t, L) = \langle m^2 \rangle^2 / \langle m^4 \rangle = \langle \sum_i c_i^2 \rangle^2 / \left\langle 3 \left(\sum_i c_i^2 \right)^2 - 2 \sum_i c_i^4 \right\rangle. \qquad (7)$$

This definition can also be used for $q \neq 2$ Potts and random-cluster models, including the percolation model. In the scaling limit, it converges to a q-dependent universal constant. For the percolation case $q = 1$ its value has been numerically determined as $Q = 0.87057(1)$ [7].

For each bond percolation configuration, we test whether there exists closed loops wrapping around the torus defined by the periodic boundary conditions. We thus sample three wrapping probabilities R_b, R_e and R_1. R_1 is the probability that there is a cluster connection to itself spanning the x direction but not the y direction. R_b is the probability that the configuration percolates in the x and the y direction. This includes the case of percolation in a diagonal direction. R_e is the probability that the configuration wraps at least once around the torus in any direction. The universal values of these quantities are exactly known in the scaling limit as $R_b = 0.351642855$, $R_e = 0.690473725$ and $R_1 = 0.169415435$ [14].

Scullard and Jacobsen [9] used instead wrapping probabilities R_0 (no wrapping) and R_2 (wrapping in two independent directions) which are dual in self-dual lattices, so that the difference $R_d \equiv R_2 - R_0$ vanishes at the critical point. For non-self-dual planar lattices, R_d still displays rapid finite-size convergence to zero at the critical point [9].
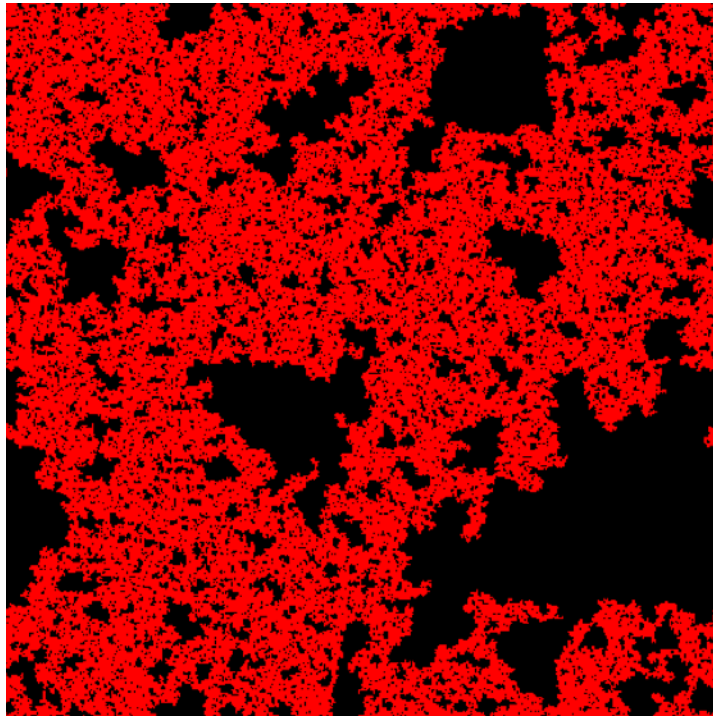
Figure 1. Typical critical configuration of the largest cluster in a 480×480 percolation model of type 1 with $z = 4$ ($r = 1$) interacting neighbors.

2.3. Finite-size scaling
According to finite-size scaling, the Binder ratio behaves as

$$Q(t, L) = Q + \sum_{j=1}^{\infty} q_j t^j L^{j y_t} + b_i L^{y_i} + b_l \ln(L) L^{y_i} + b_3 L^{d - 2y_h} + b_4 L^{y_t - 2y_h} + \cdots \qquad (8)$$

which may serve as a basis for least-squares fits to the Monte Carlo results for Q. To this purpose, we compute a set of $Q(t, L)$ data for a number of finite sizes L near the critical point. The fit may yield estimates of the critical point ($t \simeq K_c - K$), Q and y_t. It is helpful that the critical exponents are exactly known [12, 13]. Somewhat better results for the critical point may be obtained from similar fits to the results for the wrapping probabilities, because the terms with exponents $d - 2y_h$ and $y_t - 2y_h$ are absent, and the universal wrapping probabilities in the scaling limit are exactly known.

3. Results
3.1. Remarks on the nature of percolation configurations
Typical configurations of the largest cluster for lattices with size 480×480 are shown in figures 1, 2, 3 and 4, for type-1 systems with $z = 4$, 60, 4016, and the mean-field limit respectively. These figures illustrate the crossover between the uniformly distributed clusters of the mean-field model and the more sharply defined clusters of the short-range model. The density of the largest cluster decreases considerably with increasing range of interactions.
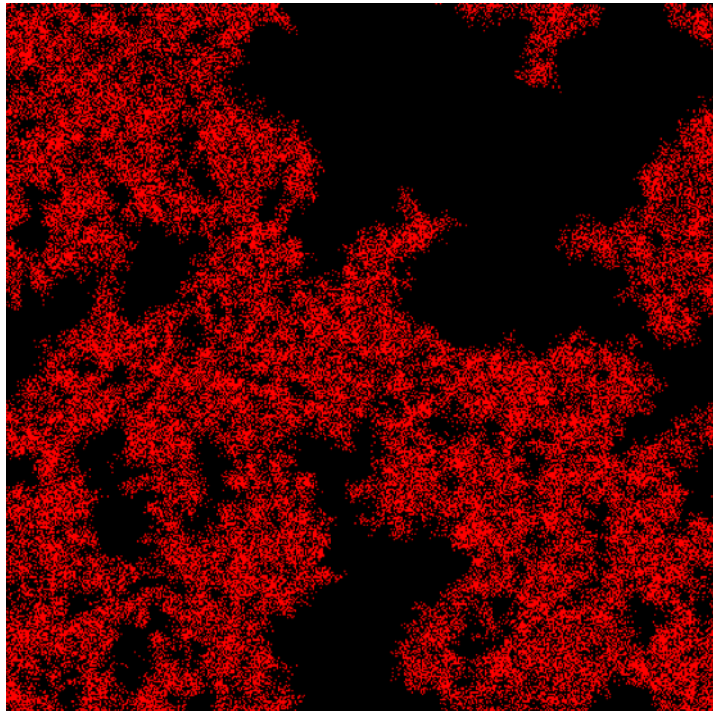
Figure 2. Typical critical configuration of the largest cluster in a 480×480 percolation model of type 1 with $z = 60$ ($r = 4.3$) interacting neighbors.
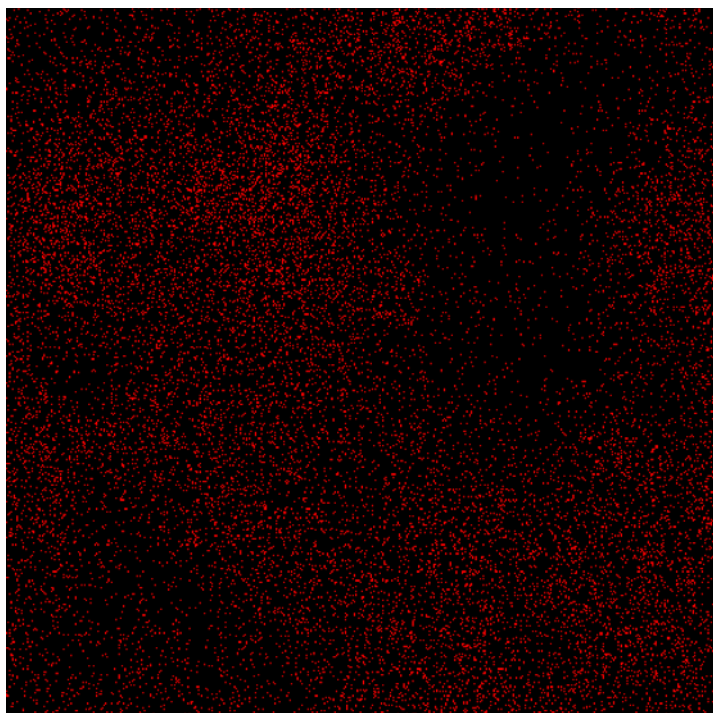

Figure 3. Typical critical configuration of the largest cluster in a 480×480 percolation model of type 1 with $z = 4016$ ($r = 35.8$) interacting neighbors.
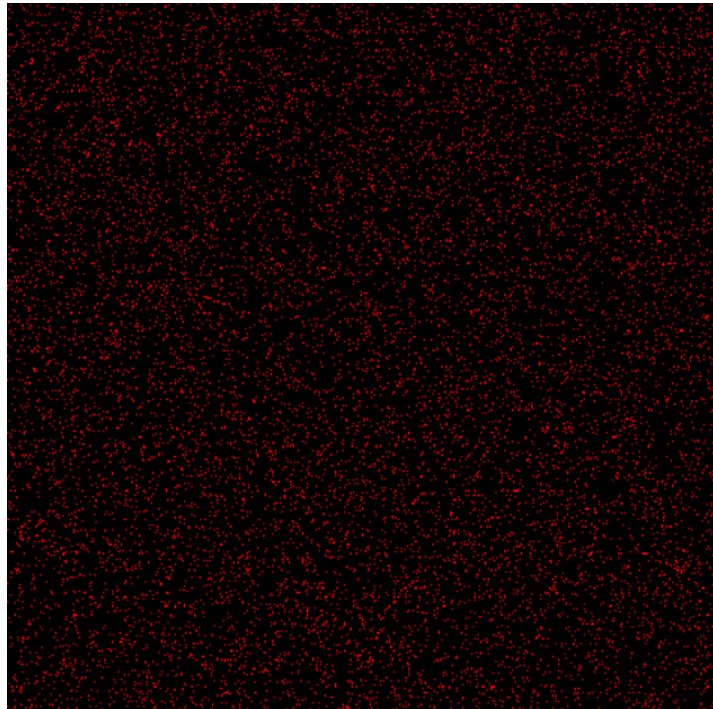
Figure 4. Typical critical configuration of the largest cluster in a 480×480 percolation model on the complete graph, i.e., the mean-field limit $r \rightarrow \infty$.

3.2. Numerical analysis of the type-1 models

The procedure used to determine the critical points, and its results for type-1 models were described in Ref. [7]. That work also determined the critical exponents and other universal quantities, and reported that all investigated models with finite z belong to the short-range percolation universality class. In this work, we extend the series of finite-range models with several additional values of the coordination number z, making use of the wrapping probability $R_{\rm d}$ defined in section 1. The results are listed in table 1.

Table 1. Results for the percolation threshold zp_c of type-1 models with several coordination numbers z. Statistical uncertainties in the last decimal place given are shown between parentheses.

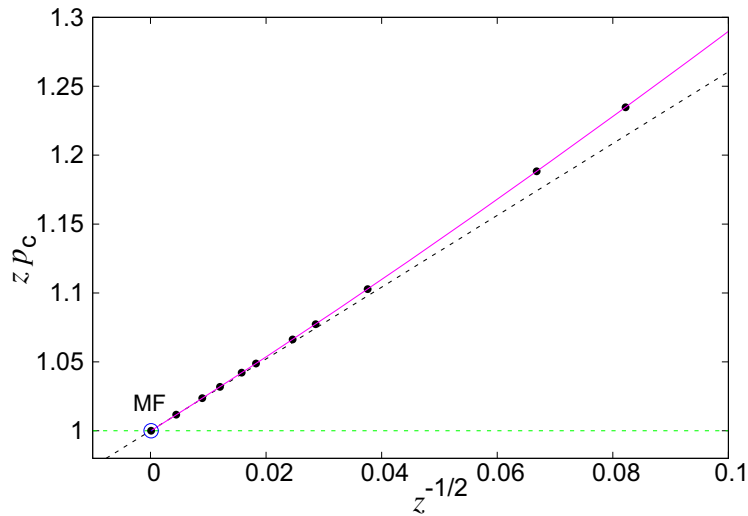| z	r	zp_c
148	7	1.234 704(2)
708	15	1.102 812(3)
1652	23	1.066 297(7)
3000	31	1.048 803(8)
4016	35.8	1.042 043(5)
6920	47	1.031 871(16)
12452	63	1.023 640(20)
50616	127	1.011 655(20)

Figure 5. Percolation threshold $p_c(z)$ versus $1/\sqrt{z}$ for type-1 models. The dashed line represents a straight line with slope 2.608, representing the first term in a fit according to $zp_c - 1 = a_1 z^{-1/2} + a_2 z^{-1} + a_3 z^{-3/2}$. The magenta curve includes all these terms.

The new data for zp_c allow a more sensitive test of its linearity as a function of $z^{-1/2}$ in comparison with Ref. [7]. We plot these critical points in figure 5 accordingly. No deviation from linearity is observable in the neighborhood of the MF point.

As a more quantitative test, we fitted the data by the expression

$$zp_c - 1 \approx (a_1 + a_2 z^{-1/2} + a_3 z^{-1})(z^{-1/2})^{1/\phi} \tag{9}$$

which did adequately describe the data for $z \geq 224$, and yielded $1/\phi = 1.002(2)$.

3.3. Numerical analysis of the type-2 models

Table 2. Results for the percolation threshold zp_c of type-2 models with several coordination numbers z. Statistical uncertainties in the last decimal place given are shown between parentheses.

z	r	zp_c
120	5	1.257 695(7)
224	7	1.184 443(5)
960	15	1.085 839(5)
2208	23	1.055 830(10)
3968	31	1.041 349(7)
9024	47	1.027 217(15)
16128	63	1.020 270(15)
65024	127	1.010 050(30)

Like for the type-1 models, the critical exponents appear to be in accurate agreement with the short-range values for all z investigated. In figure 6, the critical points of the type-2 model
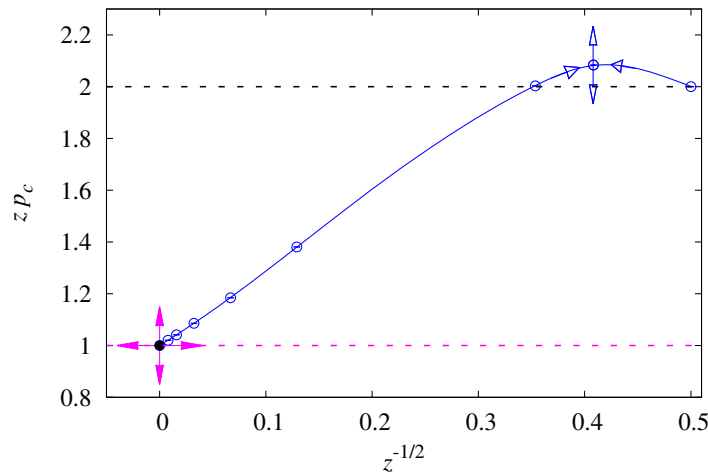
Figure 6. Critical points zp_c for type-2 equivalent-neighbor percolation models in two dimensions, and illustration of the location of the fixed points. The stable fixed point is set at the critical point $p_c = 2\sin(\pi/18)$ for the triangular-lattice bond percolation model. These results are analogous to those for type-1 models as given in Ref. [7].
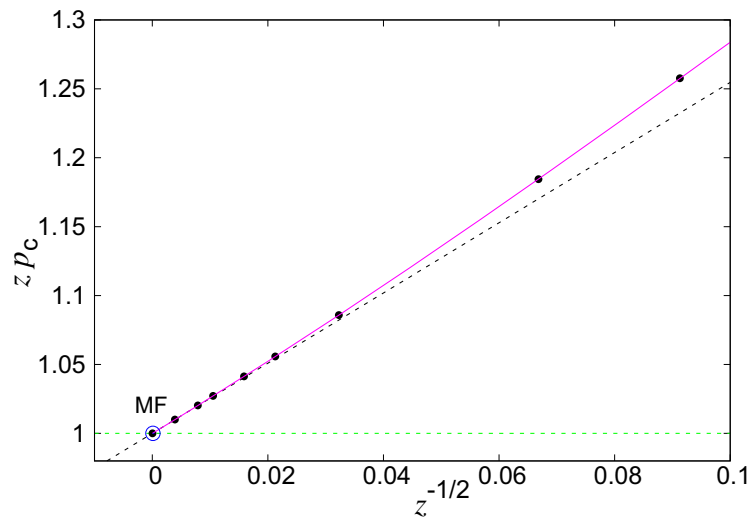

Figure 7. Percolation threshold $p_c(z)$ versus $1/\sqrt{z}$ for type-2 models.. The dashed line represents a straight line with slope 2.547, representing the first term in a fit according to $zp_c - 1 = a_1 z^{-1/2} + a_2 z^{-1} + a_3 z^{-3/2}$. The magenta curve includes all these terms.

zp_c are shown as a function of $1/\sqrt{z}$. Again, the critical points near the MF point in this figure lie approximately on a straight line. An enlarged picture is shown in figure 7. We have also fitted the type-2 critical points on the basis of Eq. (9), which yielded, after truncation, the same result $1/\phi = 1.002(2)$ as for the type-1 models.

Finally, we have constructed a data collapse of the Binder ratio Q versus L results at the critical points of the type-2 models, using a z-dependent rescaling of L. These data, together
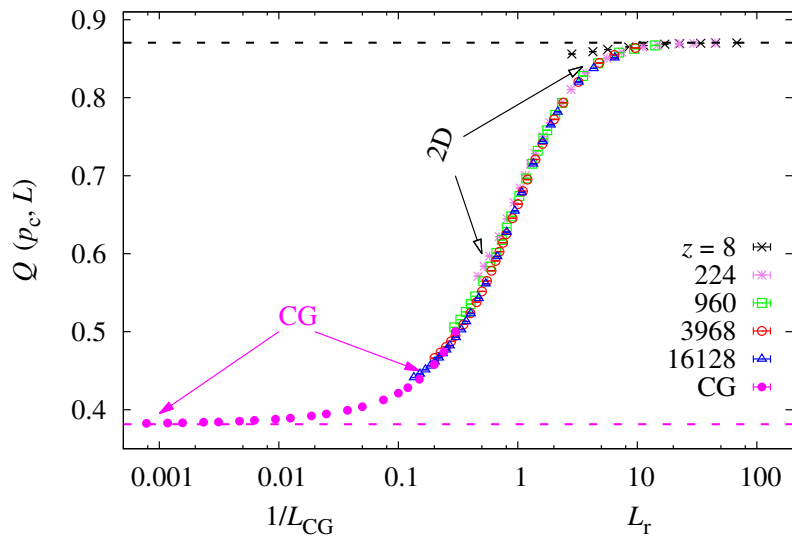
Figure 8. $Q(p_c, L)$ vs. rescaled size L_r for $z < \infty$. The rescaling factor $b(z)$ in $L_r = b(z)L$ is determined such as to collapse the finite-z data with $z > 8$ in this figure. The figure includes data for the complete graph (CG), using the inverse finite size $1/L_{CG}$ as the finite-size parameter. Dashed lines in the figure indicate the limiting values of Q for $L \to \infty$. These are 0.87057 for short-range models, and 0.38126 for the MF limit.

with finite-size results for the complete graph, cover the entire range of Q between the MF and 2D short-range fixed points. The procedure is entirely similar to that for the type-1 models analyzed in Ref. [7]. The results are also similar, but the overlap with the finite-size regime of the MF limit, while accidental and dependent on the rescaling procedure, is much larger because of the larger coordination numbers used in the present work. These results are shown in figure 8 and clearly demonstrate the crossover from the MF to the short-range behavior.

4. Conclusion
The "square" type-2 models closely follow the crossover behavior between the mean-field limit and the short-range fixed point as already found for the "almost circular" type-1 models. We confirm, with much improved accuracy, that the crossover exponent ϕ at the mean-field fixed point is equal to 1, corresponding with an exponent $y_r = 2/3$ describing the scaling of the inverse range parameter $z^{-1/2}$ at the MF fixed point [20]. We find that for the non-planar cases ($z \geq 8$), finite-size corrections in the wrapping probability R_d are, although not absent, still so small that R_d appears to be a useful quantity to determine critical points of non-planar models on the basis of Monte Carlo simulations and finite-size scaling.

References

[1] Knops H J F, van Leeuwen J M J and Hemmer P C *J. Stat. Phys.* **17** 197 (1977)

[2] Potts R B *Proc. Cambridge Philos. Soc.* **48** 106 (1952)

[3] Luijten E, Blöte H W J and Binder K *Phys. Rev.* E **54** 4626 (1996); *Phys. Rev.* E **56** 6540 (1997)

[4] Qian X F, Deng Y and Blöte H W J *Phys. Rev.* E **72** 056132 (2005)

[5] Kasteleyn P W and Fortuin C M *J. Phys. Soc. Jpn.* **26** (Suppl.) 11 (1969); Fortuin C M and Kasteleyn P W *Physica* (Amsterdam) **57** 536 (1972)

[6] Wu F Y *Rev. Mod. Phys.* **54** 235 (1982)

[7] Ouyang Y, Deng Y, and Blöte H W J submitted *Phys. Rev.* E (2018)

[8] Binder K *Z. Phys.* B **43** 119 (1981)

[9] Scullard C R and Jacobsen J L *J. Phys.* A **49** 125003 (2016), and references therein

[10] Guo W-A, Deng Y, and Blöte H W J *Phys. Rev.* E **79** 061118 (2009).

[11] Luijten E and Blöte H W J *Int. J. Mod. Phys.* C **6** 359 (1995)

[12] Nienhuis B in *Phase Transitions and Critical Phenomena* vol 11, ed C Domb and J L Lebowitz (London: Academic 1987). In Eq. (4.26) of this work, +1 has to be replaced by +2

[13] Cardy J L in *Phase Transitions and Critical Phenomena* vol 11, ed C Domb and J L Lebowitz (London: Academic 1987) p. 55, and references therein

[14] Ziff R M, Lorenz C D, and Kleban P *Physica* A **266** 17 (1999)

[15] Fisher M E, Ma S-K, and Nickel B G *Phys. Rev. Lett.* **29** 917 (1972)

[16] Sak J *Phys. Rev.* B **8** 281 (1973)

[17] Luijten E and Blöte H W J *Phys. Rev.* B **56** 8945 (1997); *Phys. Rev. Lett.* **89** 025703 (2002)

[18] Qian X F, Deng Y, Liu Y, Guo W-A, and Blöte H W J *Phys. Rev.* E **94** 052103 (2016)

[19] Nienhuis B, Berker A N, Riedel E K and Schick M *Phys. Rev. Lett.* **43** 737 (1979)

[20] Huang W, Hou P, Wang J, Ziff R M and Deng Y *Phys. Rev.* E **97** 022107 (2018)